DMD Fast Forward. Published on December 8, 2014 as DOI: 10.1124/dmd.114.060574
This article has not been copyedited and formatted. The final version may differ from this version.

Renal Xenobiotic Transporter Expression is Altered in Multiple Experimental Models of Nonalcoholic Steatohepatitis

Mark J. Canet, Rhiannon N. Hardwick, April D. Lake, Anika L. Dzierlenga, John D. Clarke, Michael J. Goedken, Nathan J. Cherrington

University of Arizona, Department of Pharmacology and Toxicology, Tucson AZ.
(M.J.C., R.N.H., A.D.L., A.L.D., J.D.C., N.J.C.)

Rutgers University, Office of Translational Science, New Brunswick NJ.
(M.J.G.)

DMD Fast Forward. Published on December 8, 2014 as DOI: 10.1124/dmd.114.060574
This article has not been copyedited and formatted. The final version may differ from this version.

Running Title: Altered Renal Drug Transporter Expression in NASH

Corresponding Author: Nathan J. Cherrington
1703 E Mabel St
Tucson AZ 85721
PH: (520) 626-0219
Fax: (520) 626-2466
cherrington@pharmacy.arizona.edu

Text Pages: 31

Abstract: 225

Introduction: 736

Discussion: 1445

References: 42

Figures: 4

Tables: 2

Abbreviations: IR, insulin resistance; HCC, hepatocellular carcinoma; MCD, methionine and choline deficient; Mrp, multidrug resistance-associated protein; NAFLD, nonalcoholic fatty liver disease; NASH, nonalcoholic steatohepatitis; Oat, organic anion transporter; Oct, organic cation transporter; P-gp, P-glycoprotein.

Abstract

Nonalcoholic fatty liver disease (NAFLD) is the most common chronic liver disease, which can progress to nonalcoholic steatohepatitis (NASH). Previous investigations have demonstrated alterations in the expression and activity of hepatic drug transporters in NASH. Moreover, studies using rodent models of cholestasis suggest that compensatory changes in kidney transporter expression occur to facilitate renal excretion during states of hepatic stress; however, little information is currently known regarding extra-hepatic regulation of drug transporters in NASH. The purpose of the current study was to investigate the possibility of renal drug transporter regulation in NASH across multiple experimental rodent models. Both rat and mouse NASH models were utilized in this investigation and include: the MCD diet, atherogenic diet, *fa/fa* rat, *ob/ob* and *db/db* mice. Histologic and pathological evaluations confirmed that the MCD and atherogenic rats as well as the *ob/ob* and *db/db* mice all developed NASH. In contrast, the *fa/fa* rats did not develop NASH but did develop extensive renal injury in comparison to the other models. Renal mRNA and protein analyses of xenobiotic transporters suggest that compensatory changes occur in NASH to favor increased xenobiotic secretion. Specifically, both apical efflux and basolateral uptake transporters are induced, whereas apical uptake transporter expression is repressed. These results suggest that NASH may alter the expression and potentially function of renal drug transporters, thereby impacting drug elimination mechanisms in the kidney.

Introduction

Nonalcoholic fatty liver disease (NAFLD) represents a range of distinct liver histopathologies ranging from simple steatosis to the more advanced nonalcoholic steatohepatitis (NASH) (Lomonaco et al., 2013). Often regarded as the hepatic manifestation of the metabolic syndrome, NAFLD is frequently accompanied by metabolic co-morbidities such as obesity, hypertension, dyslipidemia, and hyperglycemia (Ali & Cusi, 2009). Given its close association with the metabolic syndrome, the prevalence of NAFLD has quickly risen, making it the most common form of chronic liver disease in Western society (Ali & Cusi, 2009). Current estimates suggest that the worldwide prevalence of NAFLD ranges between 6%-33% and as high as 50% in certain regions and ethnic populations, whereas NASH is predicted to affect 2.7%-12.2% of the population (Lomonaco et al., 2013; Rahimi & Landaverde, 2013). Although the mechanisms are not entirely understood, it is generally well accepted that NASH pathogenesis involves several "hits", such as inflammation and oxidative stress, that may act independently or in parallel to drive disease progression (Rahimi & Landaverde, 2013; Lomonaco et al., 2013).

The role of adipocytes has recently emerged as being instrumental in the development and propagation of inflammation in NASH. In obese states, fat-laden adipocytes are a primary source for the secretion of pro-inflammatory cytokines, including tumor necrosis factor-α (TNFα), interleukin-6 (IL-6), and interleukin-1β (IL-1β), which contribute to the increased systemic levels readily observed in NASH (Hotamisligil et al., 1993; Tilg, 2010; Kochi et al., 2014). The induction of these pro-inflammatory cytokines within adipose tissue may act in a paracrine fashion by targeting

the liver and propagating the development of NASH pathogenesis (Tilg, 2010). Moreover, inflammatory mediators, particularly TNF-α, activate various intracellular signaling cascades and may contribute to the extensive dysregulation of hepatic gene expression profiles observed in the disease (Moylan et al., 2014).

A recent investigation concerning the global changes of hepatic gene expression profiles in NAFLD revealed extensive changes in the expression of drug metabolizing and membrane transporter genes in NASH (Lake et al., 2011). Indeed, NASH causes extensive alterations in the regulation of hepatic xenobiotic transporters of both human and rodent models, leading to the functional disruption of acetaminophen, ezetimibe, methotrexate, and arsenic disposition (Hardwick et al., 2012; Hardwick et al., 2011; Canet et al., 2012; Canet et al., 2014; Lickteig et al., 2007). A common observation in these studies is increased plasma retention coupled to decreased biliary elimination of xenobiotics, suggesting that patients with NASH may represent a unique population of individuals that are at higher risk of experiencing adverse drug reactions. However, little information is currently known regarding the regulation of xenobiotic transporters in distal sites during times of hepatic stress, which may further contribute to altered xenobiotic disposition in hepatic disease states.

In addition to the liver, the kidneys serve as important sites for xenobiotic excretion, and an estimated 30 % of the top 200 prescribed drugs in 2010 are eliminated by renal clearance (Morrissey et al., 2013). Studies using experimental models of cholestasis have linked liver dysfunction with compensatory responses in the regulation of xenobiotic transporters in the kidneys. Particularly, liver-specific adaptations in xenobiotic transporters occur to restrict further hepatic exposure to toxic levels of bile

acids, resulting in higher systemic levels of potentially toxic bile acids (Keppler, 2011). However, cholestatic stress also results in compensatory adaptations in the expression of renal efflux and uptake transporters that may function to facilitate the secretion of bile acids into the urine (Slitt et al., 2007; Brandoni et al., 2006b). A recent study confirmed the functional outcome of these adaptations by demonstrating increased cimetidine clearance as a result of kidney Oct2 induction in a rat model of cholestasis (Kurata et al., 2010). Together, these findings demonstrate the influence of liver dysfunction on kidney-specific handling of xenobiotics, which may impact their renal secretion.

The purpose of the current study was to investigate the effects of NASH on xenobiotic transporter expression in the kidneys. Several rodent models of NASH were utilized and a comprehensive analysis of kidney mRNA and protein expression profiles across these models was performed. These studies contribute to the hypothesis that during times of hepatic stress, compensatory alterations in kidney function occur to limit the accumulation of endogenous and exogenous compounds in systemic circulation. Moreover, these findings will change the manner in which we investigate disease-mediated effects on xenobiotic disposition by confirming that physiological adaptations occur in distal tissue sites, which can ultimately contribute to inter-individual variability in response to xenobiotics.

Materials and Methods

Materials. Tris-HCl, ethylenediaminetetraacedicacid (EDTA), sodium chloride (NaCl), glycerol, potassium phosphate (KPO_4), potassium chloride (KCl), sodium pyrophosphate (decahydrate), and Nonidet P-40 were obtained from Sigma-Aldrich (St. Louis, MO). Neutral buffered formalin (10%) was obtained from Fisher Scientific (Pittsburgh, PA).

Animals. Eight to ten week old, male, C57BL/6J, B6.Cg-Lep<ob>/J (*ob/ob*), and B6.BKS(D)-Lepr<db>/J (*db/db*) mice were obtained from Jackson Laboratories (Bar Harbor, ME). Eight to ten week old, male, Sprague Dawley and Crl:ZUC-Lepr<fa> fatty (*fa/fa*) rats were obtained from Charles River Laboratories (Wilmington, MA). All animals were acclimated in 12 hour light and dark cycles in a University of Arizona AAALAC-certified animal facility for at least one week prior to initiation of experiments and were given access to standard chow and water *ad libitum.* Housing and experimental procedures were in accordance with NIH guidelines for the care and use of experimental animals. To model NASH, C57BL/6J mice and Sprague Dawley rats (N=4) were fed either a methionine and choline deficient (MCD) diet (#518810) (Dyets, Inc., Bethlehem, PA), or an atherogenic diet (#D06061401) (Research Diets Inc., New Brunswick, NJ) for 8 weeks. As a control, C57BL/6J mice (N=4) and Sprague Dawley rats (N=4) were fed a methionine and choline re-supplemented diet (#518754) (Dyets, Inc., Bethlehem, PA). The *ob/ob* (N=4) and *db/db* (N=4) mice were fed a MCD diet for 4 weeks to induce NASH. The *fa/fa* rats were provided a modified high fat diet (#101447) for eight weeks (Dyets, Inc., Bethlehem, PA). The models chosen in this study represent a good spectrum of dietary and genetically altered animal model that have varying pathophysiological and

clinical characteristics of NASH. This allows for a more thorough and accurate analysis of the disease on renal transporter regulation. NASH pathology and liver membrane transporter expression has been characterized previously (Canet et al., 2014; Supplemental Figure 1). Moreover, a thorough review highlighting the important features of these models has been published, which the reader is encouraged to visit (Larter & Yeh, 2008)

Tissue Harvesting. At the conclusion of dietary feeding, the animals were euthanized via CO_2 asphyxiation. Liver and kidney slices for histolomorphologic examination were placed in 10% neutral-buffered formalin for 24 hours, followed by 70% ethanol. The remaining tissue was snap frozen in liquid nitrogen and stored at -80ºC for future analyses.

Tissue Staining and Evaluations. Paraffin-embedded kidney and liver sections were stained with hematoxylin and eosin (H&E) at the University of Arizona Histology Core. Kidney sections were evaluated and scored for renal injury. Liver sections were injury scored according to a previously validated NASH scoring method (Kleiner et al., 2005) and the results have been published previously (Canet et al., 2014).

RNA Purification. Total RNA was extracted and isolated from rat and mouse kidney using RNAzol B reagent (Tel-Test Inc., Friendswood, TX) per the manufacturer's protocol. RNA concentrations were determined using UV spectrophotometry, and the

integrity of the RNA was confirmed by ethidium bromide staining after agarose gel electrophoresis.

Branched DNA (bDNA) Analysis. bDNA analysis was used to determine mRNA transcript levels of transporter genes. Specific oligonucleotide probes for Mrp2, Mrp4, Mdr1a, Bcrp, Oatp1a1, Oat1, Oat3, Oct1, and Oct2 were diluted in lysis buffer supplied by the Quantigene HV Signal Amplification Kit (Genospectra, Fremont, CA). Substrate solution, lysis buffer, capture hybridization buffer, amplifier, and label probe buffer used in the analysis were all obtained from the Quantigene Discovery Kit (Genospectra). The assay was performed in 96-well format with 10 µg of total RNA added to the capture hybridization buffer and 50 µl of the diluted probe set. The total RNA was then allowed to hybridize to the probe set overnight at 53°C. Hybridization steps were performed per the manufacturer's protocol the following day. Luminescence of the samples was measured with a Quantiplex 320 bDNA luminometer interfaced with Quantiplex Data Management Software, version 5.02 (Bayer, Walpole, MA).

Protein Preparations. Whole cell lysate preparations of mouse and rat kidney were prepared from ~200 mg of tissue homogenized in NP-40 buffer (20 mM Tris HCl, 137 mM NaCl, 10% glycerol, 1% nonidet P-40, and 2 mM EDTA) with 1 Protease Inhibitor Cocktail Tablet (Roche, Indianapolis, IN) per 25 mL at 4°C. Homogenized tissue was then agitated at 4°C for 2 hours, centrifuged at 10,000 x g for 30 minutes, and the supernatant transferred to a clean collection tube. Rat kidney crude membrane fractions were prepared from ~100 mg of frozen tissue. Briefly, tissue was homogenized in

homogenization buffer (100 mM Tris HCl pH 7.4) with added Protease Inhibitor Cocktail Tablet (Roche, Indianapolis, IN) per 25 ml at 4°C. The resulting homogenate was centrifuged at 1500 x g for 10 minutes at 4°C and the supernatant was collected into ultra-centrifuge tubes and centrifuged at 100,000 x g for 70 minutes at 4°C. The resulting pellet was resuspended in 500 µl of homogenization buffer from above. Protein concentrations for both whole cell and microsomal fractions were determined using the Pierce BCA Protein Quantitation Assay (Thermo Scientific, Rockford, IL) per the manufacturer's protocol, and all samples were stored at -80ºC until further analysis.

Immunoblot Protein Analysis. Whole cell lysate or membrane fraction proteins (50 µg/well, 20 µg/well, respectively) were prepared in Laemmli sample buffer (Bio-Rad Laboratories, Hercules, CA) with or without β-mercaptoethanol and heated at 37ºC for 30 minutes prior to separation by SDS-PAGE on 7.5 % gels. Resolved protein was transferred to polyvinylidene fluoride (PVDF) or nitrocellulose membranes for 70 min at 350 mAmps at 4ºC. Following transfer, the membranes were blocked in 5 % nonfat dry milk diluted in phosphate-buffered saline-tween 20 for 1 hr at room temperature. To determine relative protein levels the following primary antibodies were used: P-gp, sc-8313; Oct1, sc-133866; Oatp1a1, sc-47265, (Santa Cruz Biotechnology, Santa Cruz, CA); Mrp2, ab15603; Mrp4, ab15602; Oat1, ab183086, (Abcam, Cambridge, MA); Bcrp, MC-981 (Kamiya Biomedical Co., Seattle, WA). The blots were incubated with primary antibody overnight at 4ºC with constant rocking. The following HRP-conjugated secondary antibodies were used: anti-rat (sc-2065), anti-rabbit (sc-2004), anti-mouse (sc-2005), and anti-goat (sc-2350 (Santa Cruz Biotechnology, Inc., Santa Cruz, CA).

Quantification of relative protein expression was determined using image processing and analysis with Image J software (NIH, Bethesda, MD) and normalized to β-actin protein (whole cell lysate) (sc-47778, Santa Cruz Biotechnology, Inc., Santa Cruz, CA) or pan-cadherin (microsomal fraction) (ab16505, Abcam, Cambridge, MA).

Statistical Analysis. Data were analyzed using one-way ANOVA to determine significant differences between model groups with a Tukey's post-hoc analysis. Histological scores were rank-ordered prior to analysis via ANOVA. A significance level of $p \leq 0.05$ was used to determine experimental significance. All analyses were carried out using GraphPad Prism software Version 5 (GraphPad Software, Inc., La Jolla, CA).

DMD Fast Forward. Published on December 8, 2014 as DOI: 10.1124/dmd.114.060574
This article has not been copyedited and formatted. The final version may differ from this version.

Results

Rodent Kidney Pathology in NASH. Histological assessments were conducted to investigate the effect of NASH on renal morphology. The incidence and severity of kidney pathology (including tubular degeneration, necrosis and regeneration, parenchymal inflammation and glomerular mesangial expansion and/or hypertrophy) are summarized in Table 1. Across the rat models, a significant increase in overall severity scores was observed in the MCD, atherogenic, and *fa/fa* animals (Figure 1C). Glomerular changes (mesangial expansion and/or hypertrophy) were the most common observation(s) in MCD and atherogenic rats, whereas the *fa/fa* rats additionally developed parenchymal tubular changes (degeneration/necrosis/regeneration, protein casts) and parenchymal inflammation (Figure 1A, arrow, inserts; Table 1). Similarly, glomerular finding were more common than tubular injury in the mouse models (Figure 1B, inserts). All mouse groups had increased overall severity scores with the exception of the *db/db* mice (Figure 1C and Table 1).

Kidney Transporter mRNA Expression in Rodent NASH. mRNA quantification analyses were conducted on renal transporter genes to determine the effect of NASH on their regulation (Figure 2 and Figure 3). The transporters chosen to be investigated in this study represent a group of important proteins that mediate the renal secretion of many xenobiotics, which include pharmaceuticals. Among the uptake transporters investigated in rats, no significant changes in gene expression were noted with the exception of Oat3, which was induced in rat MCD whereas Oatp1 was repressed in the MCD, athero, and *fa/fa* rat models (Figure 2A). In contrast, Oct2 and Oat1 were down-regulated in the

MCD, *ob/ob*, and *db/db* mice along with an induction seen in the atherogenic model (Figure 2B). Like the rats, Oat 3 was significantly induced in the *ob/ob* and *db/db* mouse models whereas Oatp1 expression was repressed in the MCD, *ob/ob* and *db/db* models and up-regulated in the atherogenic mice (Figure 2B).

In contrast to uptake transporters, efflux transporter mRNA was generally up-regulated in the rodent models with confirmed-NASH (Figure 3, Table 2). Mrp2, Mrp4, Bcrp, and Mdr1a (P-gp) genes were all induced in the rat MCD model whereas no changes were observed in the atherogenic and *fa/fa* rats (Figure 3A). Similarly, Mrp2 was induced in the *ob/ob* mice whereas Mdr1a expression was up-regulated in the MCD, atherogenic, *ob/ob* and *db/db* mouse models (Figure 3B). No changes were observed in Bcrp expression; however, Mrp4 was induced in the kidney of MCD, *ob/ob*, and *db/db* mice (Figure 3B).

Kidney Transporter Protein Expression in Rodent NASH. Protein expression of membrane transporters across rodent models was also investigated and shown in Figure 4. Consistent with the mRNA analyses, protein expression of the renal efflux transporters Mrp2 and P-gp was induced in the MCD rats (Figure 4A). In addition, P-gp expression was induced in the atherogenic rat model. Interestingly, protein expression of Bcrp was down-regulated in the kidney of *fa/fa* rats (Figure 4A). Oatp1a1, Oat1, and Oct1 renal uptake transporter expression was not significantly changed at the protein level in the rat models.

Similar to the rats, efflux transporter expression in the kidney was generally induced at the protein level in mice with NASH (Figure 4B, Table 2). Specifically, Mrp4

and P-gp protein expression was induced in the mouse MCD, *ob/ob*, and *db/db* models. Bcrp expression did not change across models except for atherogenic mice, which had a significant decrease in Bcrp protein expression in the kidney (Figure 4B). In contrast, Oatp1 protein expression was significantly reduced in the mouse *ob/ob* and *db/db* models. No change in Oat1 expression was observed in the mice; however, it tended to decrease in the *db/db* model.

Discussion

The increase in adverse drug reaction incidents has become a significant health concern worldwide. In the United States, adverse drug reactions (ADRs) have become one of the top-10 causes of death, clearly highlighting the need for more effective pharmacovigilant practices within the healthcare industry (Wooten, 2010; Valente & Murray, 2011). Many ADRs can be attributed to inter-individual variations in xenobiotic disposition, which may be preventable by identifying factors that contribute to these variations. In addition, recent advances in our understanding of the impact of disease states on xenobiotic pharmacokinetics have helped identify populations that may be at risk for developing ADRs. In particular, diseases that manifest in the liver have gained increased attention given the importance of the liver in mediating xenobiotic metabolism and disposition. Despite previous evidence demonstrating compensatory alterations in the kidney during cholestatic disease, our understanding of how NASH affects renal clearance is lacking and necessitates further investigation.

The purpose of this study was to determine the effects of NASH on the regulation of renal membrane transporters. The use of several models in these investigations allows for a more comprehensive profile that strengthens our findings and allows translating these findings to the human condition more feasible, considering it is currently unknown how the regulation of renal xenobiotic transporters is altered in human NASH. Our results demonstrate that the development of NASH causes significant alterations in the expression of several membrane transporters in the kidneys of various rodent models. In particular, we observe a coordinated up-regulation of Mrp2, Mrp4, and Pgp, suggesting that during times of hepatic stress, the kidneys may compensate by facilitating the renal

secretion of xenobiotics and endogenous substrates, such as bile acids, into the urine. Similar compensatory changes have been observed in other models of liver injury. Using bile duct-ligated mice, Slitt *et al.* demonstrated an induction of renal Mrp1-5 mRNA and a reduction in Oatp1a1 mRNA expression (Slitt et al., 2007). Interestingly, our data also show a down-regulation of renal uptake transporter Oatp1a1 expression in NASH, which facilitates the reabsorption of compounds from the renal tubule filtrate, suggesting an overall shift from renal reabsorption to renal secretion of organic anions in NASH. Furthermore, Mrp2 induction in the kidney has been observed in various rat models of cholestasis (Lee et al., 2001) as well as liver ischemia-reperfusion injury (Tanaka et al., 2008), which is consistent with our findings in the pathologically-confirmed NASH models (MCD, *ob/ob*, and *db/db* rodents).

The induction of renal Mrp2 is a common observation across several cholestatic injury models. It is proposed that Mrp2 induction in the kidneys may serve as an alternative route of elimination of bile acids in situations in which liver function is compromised (Klaassen & Aleksunes, 2010). Similar to cholestasis, hepatic Mrp2 function is significantly reduced in NASH whereas Mrp4 is induced leading to a functional shift in the disposition of xenobiotics from bile to plasma (Hardwick et al., 2012; Canet et al., 2014). The similarity in the changes to hepatic and renal transporter gene expression between cholestasis and NASH is suggestive of a common mechanism mediating these effects. Recent findings show that mice fed an MCD diet develop intrahepatic cholestasis, leading to increased plasma bile acid levels (Wu et al., 2014). Furthermore, Tanaka *et al.* has demonstrated that Mrp2 expression is elevated following treatment of renal proximal tubule cells with conjugated bilirubin or human bile

suggesting that bile acids and/or bile constituents may directly regulate Mrp2 gene transcription, possibly through the nuclear receptors farnesoid X receptor and/or pregnane X receptor (Tanaka et al., 2002;Kast et al., 2002). Together, these results demonstrate that the up-regulation of renal Mrp2 may partially be explained by direct exposure of bile acids to the kidneys due to the development of cholestasis secondary to NASH.

Similar to renal efflux transporters, the expression of Oat3 in the kidney is significantly elevated in rodents with NASH. In particular, we observe an induction of renal Oat3 in the rat MCD as well as the mouse *ob/ob* and *db/db* models. In contrast, our data suggests that Oat1 protein expression is not changed, although levels tend to decrease in the *ob/ob* and *db/db* models. This is in contrast to studies that suggest Oat1 and Oat3 are commonly coordinated together by various stressors and exogenous sressors (Guo et al., 2013;Ulu et al., 2012; Jin et al., 2012). However, consistent with our results, similar findings have been reported in experimental models of cholestasis. Chen *et al.* demonstrated an induction of Oat3 protein in the kidney whereas Oat1 levels did not change in Eisai hyperbilirubinemic (EHBR) rats, which lack functional Mrp2 and serve as a cholestatic model (Chen et al., 2008). However, Oat3 mRNA in EHBR did not change whereas we observed an induction, suggesting an alternative mechanism of regulation in NASH. Several investigations have shown that members of the Oat transporter family, in particular Oat1 and Oat3, are post-transcriptionally regulated by intracellular phosphorylation events mediated by PKC and PKA. PKC activation causes a down-regulation of Oat3-mediated uptake of estrone sulfate, whereas PKA activation leads to increased transport activity, suggesting that differential activation of protein

kinase cascades may cause tissue and disease-specific transporter regulation (Soodvilai et al., 2004). The effect of NASH on renal PKC and PKA regulation is not completely understood and further investigations are needed to clarify the mechanistic role of renal Oat3 induction in NASH.

Liver damage sustained in NASH results in inflammation, and oxidative stress, leading to hepatocellular damage. However, our results suggest that renal injury in the rodent models with NASH is minimal and lack significant evidence of inflammation and oxidative kidney injury. In contrast, the *fa/fa*, rat model, which failed to develop pathological NASH, had significant renal injury, and yet renal transporter expression in this rodent model did not vary significantly from control rats. Together, these findings suggest that direct renal injury is not a primary factor in membrane transporter regulation in NASH and that the minimal renal injury sustained in rodents with NASH may be due to liver-derived inflammation.

Alternatively, the pathological disturbances that occur in the liver may secondarily affect distal tissue function through the release of cellular mediators that may act in a paracrine signaling fashion. Chronic liver inflammation observed in NASH is associated with increased systemic levels of pro-inflammatory cytokines such as TNF-α and IL-6 (Alaaeddine et al., 2012; Kochi et al., 2014; Carter-Kent et al., 2008). Moreover, several independent studies have shown a direct role of pro-inflammatory cytokines in mediating the regulation of membrane transporters. Treatment of primary hepatocytes with TNF-α and IL-6 results in marked alterations in membrane transporter expression (Le et al., 2009b). Additionally, IL-1β exposure results in the down-regulation of membrane transporters in human hepatocytes (Le et al., 2008). Together, these findings

suggest pro-inflammatory cytokines as a potential mediator in the regulation of hepatic and renal membrane transporters in NASH. Furthermore, TNF-α and IL-6 induction in NASH may regulate renal transporter expression and function in a paracrine fashion. It has recently been shown that both TNF-α and IL-6 have differential effects on transporter expression across cell lines differing in tissue origin as well as different cell lines derived from the same tissue (Le et al., 2009a; Mosaffa et al., 2009; Malekshah et al., 2011). Further investigation is needed to characterize the differential effects of pro-inflammatory cytokines on hepatic and renal xenobiotic transporter expression in NASH.

The altered regulation of renal transporters in disease states such as cholestasis has resulted in functional disturbances in xenobiotic disposition. Induction of Oct2 in the kidney following bile duct-ligation has been shown to increase cimetidine clearance in rats (Kurata et al., 2010). Additionally, disturbances in the renal secretion of bromosulphophthalein and p-aminohippurate in rodent cholestatic models were linked to altered transporter function in the kidney (Brandoni & Torres, 2009; Brandoni et al., 2006a). However, information is lacking regarding the function of membrane transporters in the kidney during diseases such as NASH.

In conclusion, we have demonstrated that rodent models of NASH pathology cause significant alterations to membrane transporter expression in the kidney. In particular, we observe a general induction of renal apical efflux transporters as well as the basolateral uptake transporter, Oat3, whereas Oatp1 expression is significantly down-regulated. Together, these data suggest a coordinated regulation of renal membrane transporters in NASH that favors renal secretion. This may serve as an adaptive response mechanism that facilitates the elimination of xenobiotics and bile acids during times of

hepatic stress. Furthermore, our data demonstrate that the manifestation of NASH fails to cause significant pathology in the kidney, suggesting that direct tissue injury is not responsible for the changes observed in transporter regulation. These findings highlight the importance of investigating the contribution of renal elimination mechanisms during hepatic disease states.

Acknowledgements

None

Authorship Contributions

Participated in research design: Canet and Cherrington.

Conducted experiments: Canet, Hardwick, Lake, Dzierlenga, Goedken, Clarke.

Contributed new reagents:

Performed data analysis: Canet, Cherrington.

Wrote or contributed to the writing of the manuscript: Canet, Cherrington.

Reference List

Alaaeddine, N., Sidaoui, J., Hilal, G., Serhal, R., Abedelrahman, A., & Khoury, S. (2012). TNF-alpha messenger ribonucleic acid (mRNA) in patients with nonalcoholic steatohepatitis. *Eur.Cytokine Netw., 23,* 107-111.

Ali, R. & Cusi, K. (2009). New diagnostic and treatment approaches in non-alcoholic fatty liver disease (NAFLD). *Ann.Med., 41,* 265-278.

Brandoni, A., Anzai, N., Kanai, Y., Endou, H., & Torres, A. M. (2006a). Renal elimination of p-aminohippurate (PAH) in response to three days of biliary obstruction in the rat. The role of OAT1 and OAT3. *Biochim.Biophys.Acta, 1762,* 673-682.

Brandoni, A. & Torres, A. M. (2009). Characterization of the mechanisms involved in the increased renal elimination of bromosulfophthalein during cholestasis: involvement of Oatp1. *J.Histochem.Cytochem., 57,* 449-456.

Brandoni, A., Villar, S. R., Picena, J. C., Anzai, N., Endou, H., & Torres, A. M. (2006b). Expression of rat renal cortical OAT1 and OAT3 in response to acute biliary obstruction. *Hepatology, 43,* 1092-1100.

Canet, M. J., Hardwick, R. N., Lake, A. D., Dzierlenga, A. L., Clarke, J. D., & Cherrington, N. J. (2014). Modeling human nonalcoholic steatohepatitis-associated changes in drug transporter expression using experimental rodent models. *Drug Metab Dispos., 42,* 586-595.

Canet, M. J., Hardwick, R. N., Lake, A. D., Kopplin, M. J., Scheffer, G. L., Klimecki, W. T. et al. (2012). Altered arsenic disposition in experimental nonalcoholic fatty liver disease. *Drug Metab Dispos., 40,* 1817-1824.

Carter-Kent, C., Zein, N. N., & Feldstein, A. E. (2008). Cytokines in the pathogenesis of fatty liver and disease progression to steatohepatitis: implications for treatment. *Am.J.Gastroenterol., 103,* 1036-1042.

Chen, J., Terada, T., Ogasawara, K., Katsura, T., & Inui, K. (2008). Adaptive responses of renal organic anion transporter 3 (OAT3) during cholestasis. *Am.J.Physiol Renal Physiol, 295,* F247-F252.

Guo, X., Meng, Q., Liu, Q., Wang C., Sun, H., Peng, J. et al. (2013). JBP485 improves gentamicin-induced acute renal failure by regulating the expression and function of Oat1 and Oat3 in rats. *Toxicol.Appl.Pharmacol., 271*, 285-295.

Hardwick, R. N., Fisher, C. D., Canet, M. J., Lake, A. D., & Cherrington, N. J. (2010). Diversity in antioxidant response enzymes in progressive stages of human nonalcoholic fatty liver disease. *Drug Metab Dispos., 38,* 2293-2301.

Hardwick, R. N., Fisher, C. D., Canet, M. J., Scheffer, G. L., & Cherrington, N. J. (2011). Variations in ATP-binding cassette transporter regulation during the progression of human nonalcoholic fatty liver disease. *Drug Metab Dispos., 39,* 2395-2402.

Hardwick, R. N., Fisher, C. D., Street, S. M., Canet, M. J., & Cherrington, N. J. (2012). Molecular mechanism of altered ezetimibe disposition in nonalcoholic steatohepatitis. *Drug Metab Dispos., 40,* 450-460.

Hotamisligil, G. S., Shargill, N. S., & Spiegelman, B. M. (1993). Adipose expression of tumor necrosis factor-alpha: direct role in obesity-linked insulin resistance. *Science, 259,* 87-91.

Jin, L., Kikuchi, R., Saji, T., Kusuhara, H., Sugiyama, Y., (2012). Regulation of tissue-specific expression of renal organic anion transporters by hepatocyte nuclear facor 1 α/β and DNA methylation. *J.Pharmacol.Exp.Ther.,40,* 648-655.

Kast, H. R., Goodwin, B., Tarr, P. T., Jones, S. A., Anisfeld, A. M., Stoltz, C. M. et al. (2002). Regulation of multidrug resistance-associated protein 2 (ABCC2) by the nuclear receptors pregnane X receptor, farnesoid X-activated receptor, and constitutive androstane receptor. *J.Biol.Chem., 277,* 2908-2915.

Keppler, D. (2011). Cholestasis and the role of basolateral efflux pumps. *Z.Gastroenterol., 49,* 1553-1557.

Klaassen, C. D. & Aleksunes, L. M. (2010). Xenobiotic, bile acid, and cholesterol transporters: function and regulation. *Pharmacol.Rev., 62,* 1-96.

Kochi, T., Shimizu, M., Terakura, D., Baba, A., Ohno, T., Kubota, M. et al. (2014). Non-alcoholic steatohepatitis and preneoplastic lesions develop in the liver of

obese and hypertensive rats: suppressing effects of EGCG on the development of liver lesions. *Cancer Lett., 342,* 60-69.

Kurata, T., Muraki, Y., Mizutani, H., Iwamoto, T., & Okuda, M. (2010). Elevated systemic elimination of cimetidine in rats with acute biliary obstruction: the role of renal organic cation transporter OCT2. *Drug Metab Pharmacokinet., 25,* 328-334.

Lake, A. D., Novak, P., Fisher, C. D., Jackson, J. P., Hardwick, R. N., Billheimer, D. D. et al. (2011). Analysis of global and absorption, distribution, metabolism, and elimination gene expression in the progressive stages of human nonalcoholic fatty liver disease. *Drug Metab Dispos., 39,* 1954-1960.

Le, V. M., Gripon, P., Stieger, B., & Fardel, O. (2008). Down-regulation of organic anion transporter expression in human hepatocytes exposed to the proinflammatory cytokine interleukin 1beta. *Drug Metab Dispos., 36,* 217-222.

Le, V. M., Lecureur, V., Moreau, A., Stieger, B., & Fardel, O. (2009a). Differential regulation of drug transporter expression by hepatocyte growth factor in primary human hepatocytes. *Drug Metab Dispos., 37,* 2228-2235.

Le, V. M., Lecureur, V., Stieger, B., & Fardel, O. (2009b). Regulation of drug transporter expression in human hepatocytes exposed to the proinflammatory cytokines tumor necrosis factor-alpha or interleukin-6. *Drug Metab Dispos., 37,* 685-693.

Lee, J., Azzaroli, F., Wang, L., Soroka, C. J., Gigliozzi, A., Setchell, K. D. et al. (2001). Adaptive regulation of bile salt transporters in kidney and liver in obstructive cholestasis in the rat. *Gastroenterology, 121,* 1473-1484.

Larter, C. Z. & Yeh, M. M. (2008). Animal models of NASH: getting both pathology and metabolic context right. *J Gastroenterol.Hepatol., 23,* 1635-1648.

Lickteig, A. J., Fisher, C. D., Augustine, L. M., Aleksunes, L. M., Besselsen, D. G., Slitt, A. L. et al. (2007). Efflux transporter expression and acetaminophen metabolite excretion are altered in rodent models of nonalcoholic fatty liver disease. *Drug Metab Dispos., 35,* 1970-1978.

Lomonaco, R., Sunny, N. E., Bril, F., & Cusi, K. (2013). Nonalcoholic fatty liver disease: current issues and novel treatment approaches. *Drugs, 73,* 1-14.

Malekshah, O. M., Bahrami, A. R., Afshari, J. T., Mosaffa, F., & Behravan, J. (2011). Correlation between PXR and ABCG2 patterns of mRNA expression in a MCF7 breast carcinoma cell derivative upon induction by proinflammatory cytokines. *DNA Cell Biol., 30,* 25-31.

Morrissey, K. M., Stocker, S. L., Wittwer, M. B., Xu, L., & Giacomini, K. M. (2013). Renal transporters in drug development. *Annu.Rev.Pharmacol.Toxicol., 53,* 503-529.

Mosaffa, F., Lage, H., Afshari, J. T., & Behravan, J. (2009). Interleukin-1 beta and tumor necrosis factor-alpha increase ABCG2 expression in MCF-7 breast

carcinoma cell line and its mitoxantrone-resistant derivative, MCF-7/MX. *Inflamm.Res., 58,* 669-676.

Moylan, C. A., Pang, H., Dellinger, A., Suzuki, A., Garrett, M. E., Guy, C. D. et al. (2014). Hepatic gene expression profiles differentiate presymptomatic patients with mild versus severe nonalcoholic fatty liver disease. *Hepatology, 59,* 471-482.

Rahimi, R. S. & Landaverde, C. (2013). Nonalcoholic fatty liver disease and the metabolic syndrome: clinical implications and treatment. *Nutr.Clin.Pract., 28,* 40-51.

Slitt, A. L., Allen, K., Morrone, J., Aleksunes, L. M., Chen, C., Maher, J. M. et al. (2007). Regulation of transporter expression in mouse liver, kidney, and intestine during extrahepatic cholestasis. *Biochim.Biophys.Acta, 1768,* 637-647.

Soodvilai, S., Chatsudthipong, V., Evans, K. K., Wright, S. H., & Dantzler, W. H. (2004). Acute regulation of OAT3-mediated estrone sulfate transport in isolated rabbit renal proximal tubules. *Am.J.Physiol Renal Physiol, 287,* F1021-F1029.

Tanaka, Y., Chen, C., Maher, J. M., & Klaassen, C. D. (2008). Ischemia-reperfusion of rat livers decreases liver and increases kidney multidrug resistance associated protein 2 (Mrp2). *Toxicol.Sci., 101,* 171-178.

Tanaka, Y., Kobayashi, Y., Gabazza, E. C., Higuchi, K., Kamisako, T., Kuroda, M. et al. (2002). Increased renal expression of bilirubin glucuronide transporters in a rat model of obstructive jaundice. *Am.J.Physiol Gastrointest.Liver Physiol, 282,* G656-G662.

Tilg, H. (2010). The role of cytokines in non-alcoholic fatty liver disease. *Dig.Dis., 28,* 179-185.

Ulu, R., Dogukan, A., Tuzcu, M., Gencoglu, H., Ulas, M., Ihan, N. et al. (2012) Regulation of renal organic anion and cation transporters by thymoquinine in cisplatin induced kidney injury. *Food.Chem.Toxicol., 50,* 1675-1679.

Valente, S. & Murray, L. P. (2011). Creative strategies to improve patient safety: allergies and adverse drug reactions. *J.Nurses Staff.Dev., 27,* E1-E5.

Wooten, J. M. (2010). Adverse drug reactions: Part I. *South.Med.J., 103,* 1025-1028.

Wu, W., Liu, X., Peng, X., Xue, R., Ji, L., Shen, X. et al. (2014). Bile acids override steatosis in farnesoid X receptor deficient mice in a model of non-alcoholic steatohepatitis. *Biochem.Biophys.Res.Commun., 448,* 50-55.

DMD Fast Forward. Published on December 8, 2014 as DOI: 10.1124/dmd.114.060574
This article has not been copyedited and formatted. The final version may differ from this version.

Footnotes

This work was supported by National Institutes of Health grants [AI083927], [ES006694], [HD062489], National Institute of Environmental Health Science Toxicology Training Grant [ES007091], and The National Science Foundation of Arizona.

Address correspondence to: Nathan J. Cherrington, Ph.D., Department of Pharmacology and Toxicology, College of Pharmacy, University of Arizona, 1703 East Mabel, Tucson, AZ 85721, Email: cherrington@pharmacy.arizona.edu

DMD Fast Forward. Published on December 8, 2014 as DOI: 10.1124/dmd.114.060574
This article has not been copyedited and formatted. The final version may differ from this version.

Figure Legends

Figure 1. Kidney Histology in Rodent NASH. Representative hematoxylin and eosin stained kidney sections from rat (A) and mouse (B) NASH models. A significant number of protein casts was present in the kidneys of *fa/fa* rats (2A; arrow). Images were taken at 20X magnification. . Higher magnification (100X) images of glomerular changes were captured and shown as an insert to each figure. Pathological scoring evaluations describing total kidney injury scores (C) are shown. Horizontal bar represents the median of data (N=4 animals) and * $p \leq 0.05$ versus control within each group. Data was ranked-ordered prior to statistical analysis. Scoring key: 0- none; 1- minimal (<10% affected); 2- mild (10-25% affected); 3- moderate (25-40% affected); 4- marked (40-50% affected); 5- severe (>50% affected).

Figure 2. Kidney Uptake Transporter mRNA Expression in Rodent NASH. mRNA expression of rat uptake (A) and mouse uptake (B) transporters in the kidneys of rodent NASH models via bDNA gene analysis. The transporters investigated, with the exception of Oatp1a1, are localized on the basolateral membrane of renal proximal tubules and participate in the uptake of substrates from the peritubular capillaries into the proximal tubule cell for secretion into to lumen for urinary secretion. In contrast, Oatp1a1 is expressed on the apical membrane of the proximal tubule cell and is responsible for the uptake of substrates into the proximal tubule cell from the lumen filtrate in a process known as re-absoption. Data represent the mean ± S.E.M from 4 animals. * $p \leq 0.05$ versus control within each group.

Figure 3. Kidney Efflux Transporter mRNA Expression in Rodent NASH. mRNA expression of rat efflux (A) and mouse efflux (B) transporters in the kidneys of rodent NASH models via bDNA gene analysis. The efflux transporters investigated are localized on the apical membrane of renal proximal tubule cells and participate in the efflux of substrates directly into the nephron lumen for urinary excretion. Data represent the mean ± S.E.M from 4 animals. * $p \leq 0.05$ versus control within each group.

Figure 4. Kidney Protein Expression of Membrane Transporters in Rodent NASH. Western blot analyses depicting rat (A) and mouse (B) transporter expression in the kidneys of rodent NASH models. Densitometry analysis and representative Western blots are shown. β-actin was used a loading control for whole cell lysates, whereas pan-cadherin was used for crude membrane preparations. Rat Mrp2 and Oct1 protein were analyzed using crude membrane preparations whereas the remainder (mouse and rat) were analyzed in whole cell fractions. Data represent the mean ± S.E.M from 4 animals. * $p \leq 0.05$ versus control within each group.

Table 1: Kidney Pathology Scoring in NASH Models

Kidney pathology was assessed via the lesions described below. Values represent the median (range) of N=4 animals and were rounded to next whole number (median of 1.5 is reported as 2). Scoring key: 0- none; 1- minimal (<10% affected); 2- mild (10-25% affected); 3- moderate (25-40% affected); 4- marked (40-50% affected); 5- severe (>50% affected).

		Tubular Degeneration	Necrosis	Regeneration	Inflammation	Mesangial Expansion	Glomerular Hypertrophy
Rats	Control	0 (0)	0 (0)	0 (0)	0 (0)	0 (0)	0 (0)
	MCD	0 (0)	0 (0)	0 (0)	0 (0)	**1** (1-2)	0 (0)
	Athero	0 (0)	0 (0)	0 (0)	0 (0)	**1** (1-2)	0 (0)
	fa/fa	**1** (1)	**1** (0-1)	**2** (1-2)	**1** (0-1)	**3** (2-4)	**1** (0-1)
Mice	Control	0 (0)	0	0 (0)	0 (0)	0 (0)	0 (0)
	MCD	0 (0-1)	0	**1** (0-1)	0 (0)	**1** (1)	0 (0-1)
	Athero	0 (0)	0	0 (0)	0 (0)	**1** (1)	0 (0-1)
	ob/ob	0 (0)	0	0 (0)	0 (0)	**1** (1)	0 (0-1)
	db/db	0 (0)	0 (0-1)	0 (0)	0 (0)	**1** (1)	**1** (0-1)

Table 2: Summary of mRNA and Protein Transporter Changes

Table summarizing the overall changes in mRNA and protein expression of renal membrane transporters across rodent models with NASH. NC = no change; ND = not done.

Transporter	mRNA	Protein
Mrp2	↑	↑
Mrp4	↑	↑ (MOUSE)
P-gp	↑	↑
Bcrp	↑ (RAT)	NC
Oat1	↓ (MOUSE)	NC
Oat3	↑	ND
Oct1	NC	NC
Oct2	↓ (MOUSE)	ND
Oatp1a1	↓	↓ (MOUSE)

Figure 1

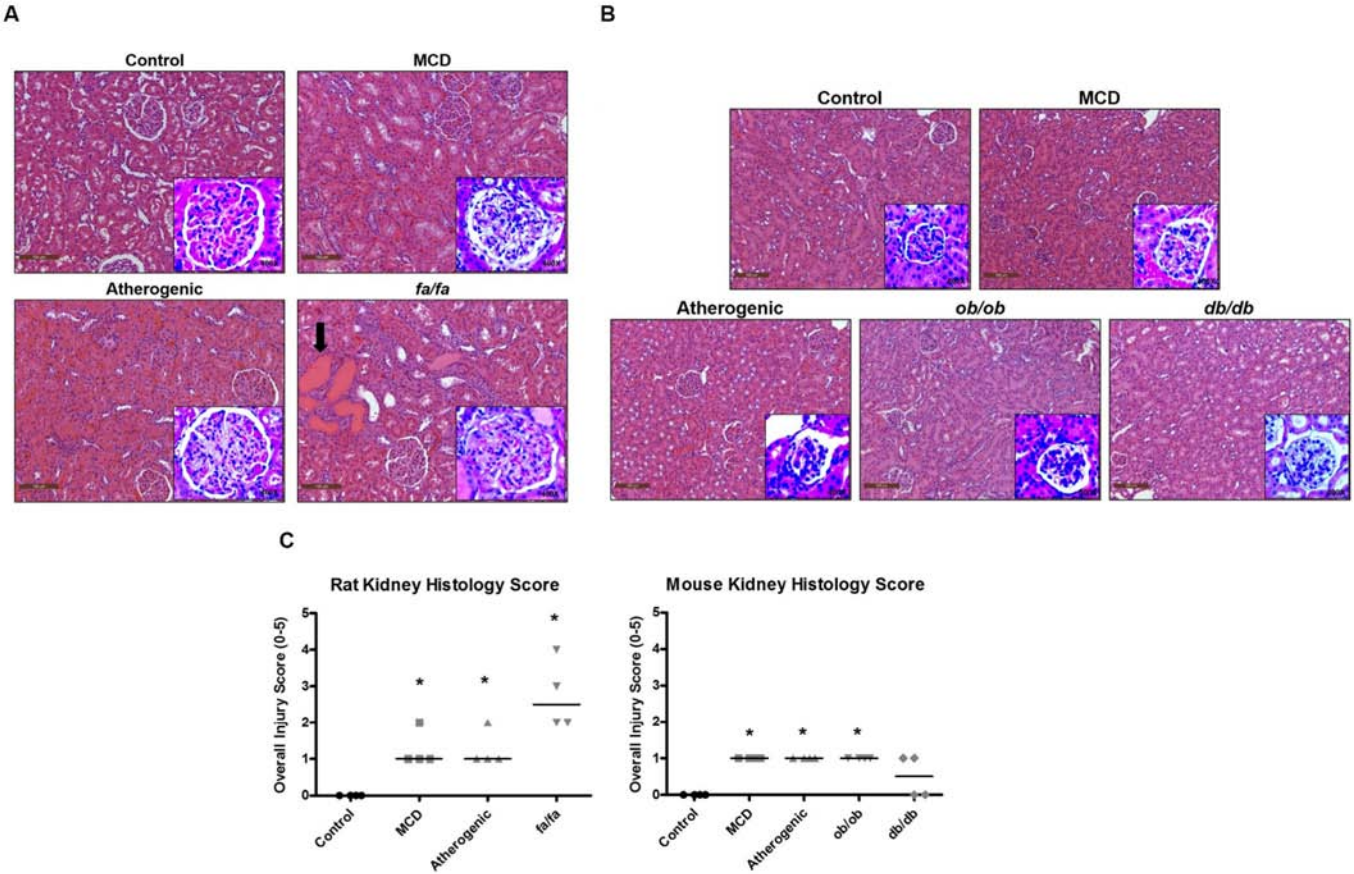
A
Control
MCD
Atherogenic
fa/fa
B
Control
MCD
Atherogenic
ob/ob
db/db
C
Rat Kidney Histology Score
Overall Injury Score (0-5)
Control
MCD
Atherogenic
fa/fa
Mouse Kidney Histology Score
Overall Injury Score (0-5)
Control
MCD
Atherogenic
ob/ob
db/db

Figure 2

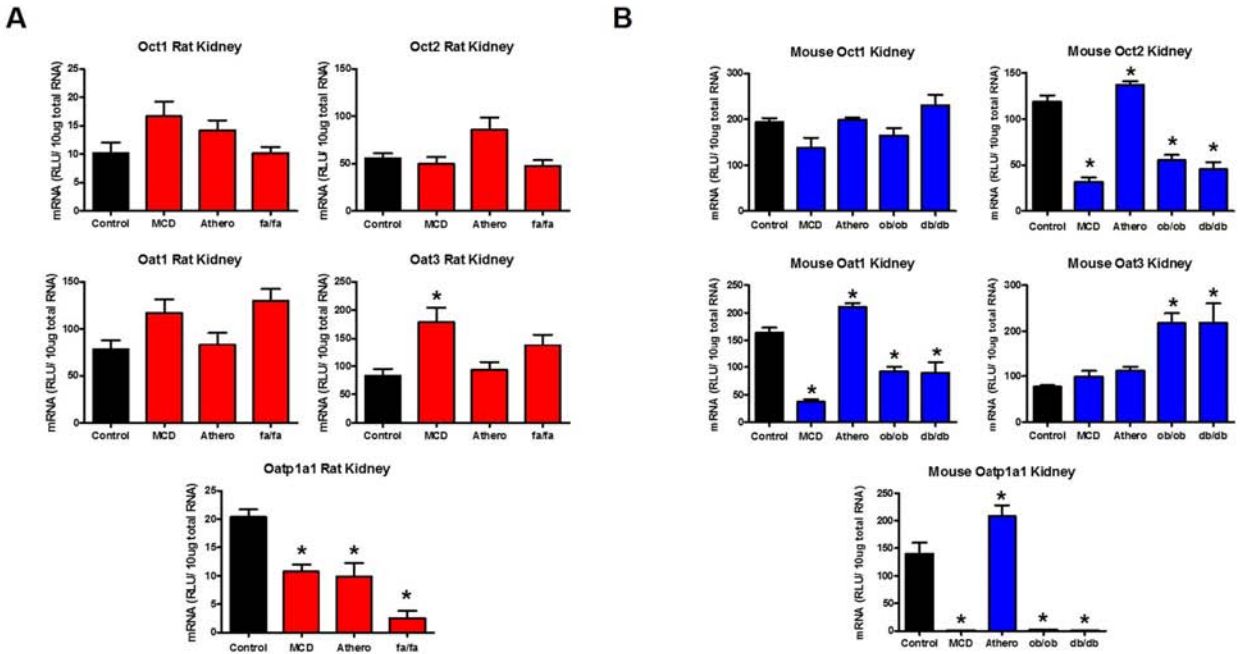
A
Oct1 Rat Kidney
Oct2 Rat Kidney
Oat1 Rat Kidney
Oat3 Rat Kidney
Oatp1a1 Rat Kidney
mRNA (RLU/ 10ug total RNA)
Control
MCD
Athero
fa/fa
B
Mouse Oct1 Kidney
Mouse Oct2 Kidney
Mouse Oat1 Kidney
Mouse Oat3 Kidney
Mouse Oatp1a1 Kidney
ob/ob
db/db

Figure 3

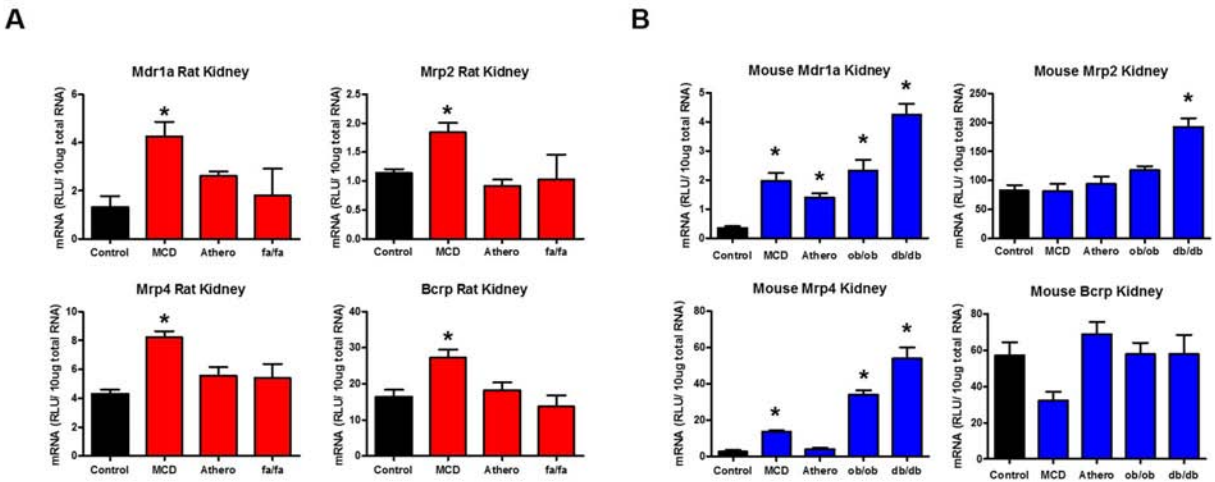
A
Mdr1a Rat Kidney
Mrp2 Rat Kidney
Mrp4 Rat Kidney
Bcrp Rat Kidney
mRNA (RLU/ 10ug total RNA)
Control
MCD
Athero
fa/fa
B
Mouse Mdr1a Kidney
Mouse Mrp2 Kidney
Mouse Mrp4 Kidney
Mouse Bcrp Kidney
mRNA (RLU/ 10ug total RNA)
Control
MCD
Athero
ob/ob
db/db

Figure 4

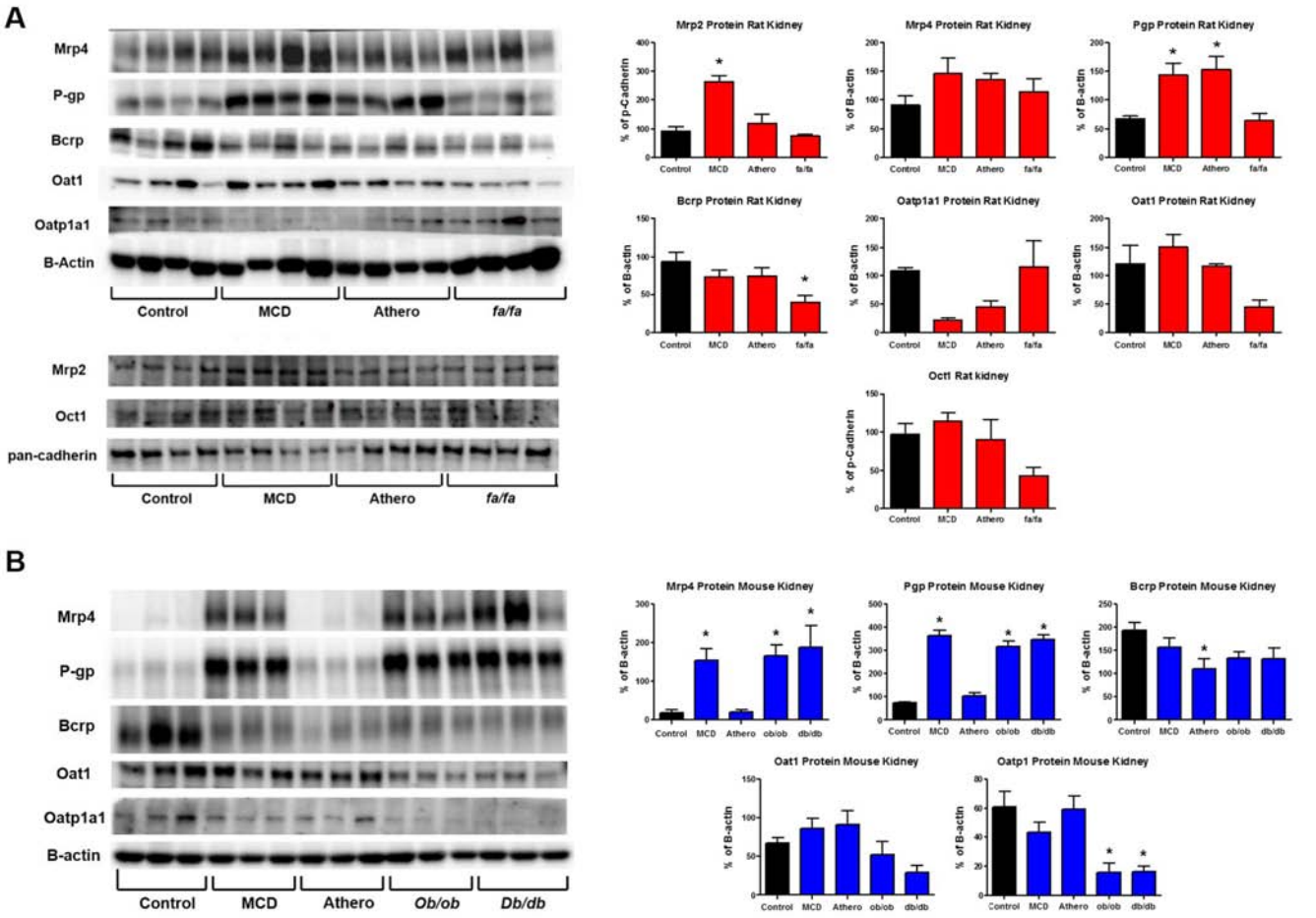
A
Mrp4
P-gp
Bcrp
Oat1
Oatp1a1
B-Actin
Control
MCD
Athero
fa/fa
Mrp2
Oct1
pan-cadherin
Control
MCD
Athero
fa/fa
Mrp2 Protein Rat Kidney
% of p-Cadherin
Mrp4 Protein Rat Kidney
% of B-actin
Pgp Protein Rat Kidney
% of B-actin
Bcrp Protein Rat Kidney
% of B-actin
Oatp1a1 Protein Rat Kidney
% of B-actin
Oat1 Protein Rat Kidney
% of B-actin
Oct1 Rat kidney
% of p-Cadherin
B
Mrp4
P-gp
Bcrp
Oat1
Oatp1a1
B-actin
Control
MCD
Athero
Ob/ob
Db/db
Mrp4 Protein Mouse Kidney
% of B-actin
Pgp Protein Mouse Kidney
% of B-actin
Bcrp Protein Mouse Kidney
% of B-actin
Oat1 Protein Mouse Kidney
% of B-actin
Oatp1 Protein Mouse Kidney
% of B-actin
Control
MCD
Athero
ob/ob
db/db